Photon drag effect in carbon nanotube yarns

Alexander N. Obraztsov,[1,2] Dmitry A. Lyashenko,[1] Shaoli Fang,[3] Ray H. Baughman,[3] Petr A. Obraztsov,[1,4] Sergei V. Garnov,[4] and Yuri P. Svirko[1,a]

[1]*Department of Physics and Mathematics, University of Joensuu, Joensuu 80101, Finland*
[2]*Department of Physics, Moscow State University, Moscow 119991, Russia*
[3]*Alan G. MacDiarmid NanoTech Institute, University of Texas at Dallas, Richardson, Texas 75083, USA*
[4]*A.M. Prokhorov General Physics Institute, Russian Academy of Science, Moscow 119991, Russia*

We demonstrate that in graphitic nanocarbon materials, combination of ballistic conductivity and strong electron photon coupling opens a unique opportunity to observe transfer of momentum of the electromagnetic radiation to free carriers. The resulting drag of quasiballistically propagating electrons can be employed, in particular, to visualize the temporal profile, polarization, and propagation direction of the laser pulse. In this letter, we report the giant photon drag effect in yarns made of multiwall carbon nanotubes. © *2009 American Institute of Physics.*
[DOI: 10.1063/1.3151834]

Carbon nanotubes and graphene have recently attracted a great deal of attention as prospective materials for nanoscale electronics,[1,2] and as a unique playground for studying carriers' dynamics in the system with reduced dimensionality and nonparabolic band structure.[3,4] Although anomalous electron mobility and the ballistic current carrying capability are heavily hampered by inevitably large contact resistance, the submicron free pass and very low electron momentum relaxation rate make these materials with dominating sp^2 bonding interesting for spintronics[5] and optoelectronics.[2] Here we demonstrate that in graphitic nanocarbons, combination of quasiballistic conductivity and strong electron-photon coupling[6–8] opens a unique opportunity to observe transfer of momentum of the electromagnetic radiation to free carriers in solids.[9] This phenomenon is referred to as photon drag effect and manifests itself as a direct current (dc) generated in the conductive material as a result of its illumination by intense laser radiation. We show that in nanowires made of carbon nanotubes, this effect gives rise to the strong dc signal under irradiation with the nanosecond light pulses.

In the experiment, we employed multiwall carbon nanotube (MWNT) twisted yarns prepared using methods described elsewhere.[10] Singles yarns, about 5 μm in diameter, were drawn from a nanotube forest during the introduction of roughly 80 000 turns/m twist, and then the singles yarns were plied to make two ply yarns (see Fig. 1). About 200 000 MWNTs preferentially aligned along the yarn axis pass through the cross-section of such two ply yarn. In the experiment, we employed seven 12 mm long parallel yarns placed on a glass substrate between two electrodes [Fig. 2(a)]. The electric resistance between the electrodes was about 70 Ω and the interelectrode capacitance was less than 1 pF. The substrate was attached to the rotating stage to control orientation of the MWNT yarns with respect to the incident laser beam.

The MWNT yarns on glass substrate were irradiated using 10 ns long laser pulses, which had energy up to 20 mJ and a repetition rate of 10 Hz at a wavelength of 1600 nm. The *p*-polarized laser beam had a diameter of 4 mm. The irradiated surface area of the MWNT yarns varied from 0.2 to 0.8 mm^2 depending on the angle of incidence. The experimental setup schematically shown in Fig. 2(b) allowed us to change the incidence (α) and azimuth (β) angles of the laser beam with respect to the sample surface. We found that laser pulse produces electric potential between the opposite ends of the irradiated MWNT yarns. The voltage generated between the electrodes was measured by an oscilloscope with bandwidth of 400 MHz connected to the electrodes. The temporal profile of the electric signal was virtually identical to that of the incident laser pulse measured by an InGaAs photodiode.

The results of measurements performed at the pulse energy of 18 mJ are presented in Fig. 3. The magnitude of the electric pulse is an odd function of the angle of incidence α with maximum at $\alpha \approx 50°$ [see Fig. 3(a)] and is proportional to $\cos \beta$, where β is the azimuth angle between the incidence plane and the normal to the electrodes [see Fig. 3(b)]. Such an angular dependence of the light-induced signal can be understood if one recalls that the photon drag current in the yarn is determined by the light flux **S** along the yarn axis **l**, $J \propto (l S)$. By taking into account transmittivity of the yarn-vacuum interface, $T = 4n \, |\cos \alpha / (\cos \alpha + \sqrt{n^2 - \sin^2 \alpha})|^2$, where n is the effective refractive index of the yarn. The equation for the photon drag current can be presented in the
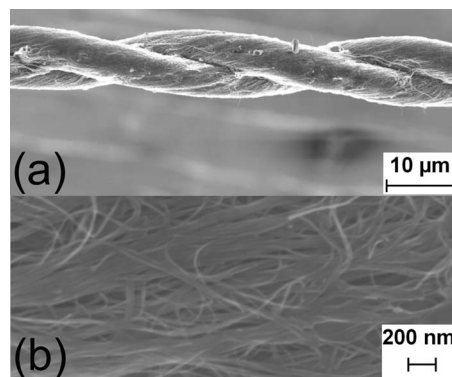

FIG. 1. (a) SEM image of two-ply MWNT yarn obtained by overtwisting singles yarn. (b) SEM image of a single yarn surface at higher magnification. One can observe MWNTs aligned along the yarn axis.
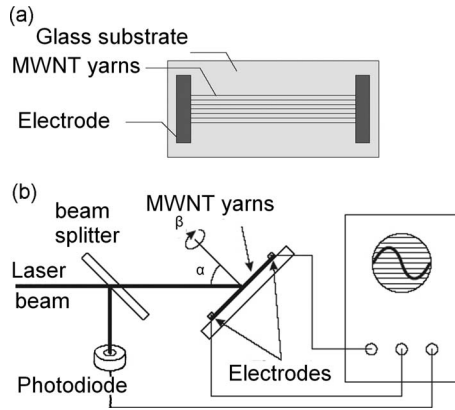
a)Electronic mail: yuri.svirko@joensuu.fi.

FIG. 2. (a) Schematic presentation of the measured sample, which contains seven two-ply, 12 mm long parallel MWNT yarns placed on a glass substrate between two electrodes. (b) Experimental setup. The sample was attached to the rotating stage that allows us to control the incidence (α) and azimuth (β) angles of the laser beam with respect to the sample surface.

following form: $J=aIT \sin \alpha \cos \beta$, where a is a material parameter and I is the light intensity. Therefore, the angular dependence of the light-induced voltage, $U=J\rho d/\cos \alpha$, where ρ is the resistance of the yarn per unit length, is given by $U \propto \sin 2\alpha \cos \beta/|\cos \alpha+\sqrt{n^2-\sin^2 \alpha}|^2$. One can observe from this equation that at $|n| \gg 1$, the signal is proportional to $\sin 2\alpha \cos \beta$. However, a finite value of refraction index gives rise to a slight shift in the maximum. In our experimental conditions, maximum of the photon drag signal is observed at $\alpha \approx 50°$ rather than at $\alpha=45°$.

The amplitude of the electric pulse generated in the MWNT yarns at $\alpha=+50°$ and $\beta=0°$ is a linear function of the incident pulse power with the slope of about 750 mV/MW. The sign of the signal was reversed when the incidence angle changed from $\alpha=+50°$ to $\alpha=-50°$, indicating that the observed phenomenon does not originate from the Dember effect occurring due to spatial inhomogeneity of photoexcited carriers.[11]

The angular dependence of the light-induced dc signal in MWNT yarns resembles that in nanographite film, in which this phenomenon was described in terms of optical rectification effect[12,13] on the quadrupole second-order nonlinearity.[14] However, when free carriers dominate the light-induced dc response, e.g., in metal and semiconductors, this phenomenon can be seen as a manifestation of the photon drag effect.[9,15,16] This effect arises from the transfer of momentum from photons to free carriers in an absorption process mediated by the electron-phonon coupling. In this process, free carriers acquire a directed motion caused by the absorbed photon momentum. Thus similarly to the optical rectification effect on the second-order quadrupole nonlinearity, the photon drag effect is entirely due to a momentum carried by the light wave. The participation of the phonons in the process of photon momentum transfer is required by the energy and momentum conservation laws, and implies a strong electron-phonon coupling. On the other hand, the light-induced current exists only during the momentum relaxation time, which is also determined by the electron-phonon coupling. The strong electron-phonon coupling gives rise to a higher photon momentum transfer rate and to shorter momentum relaxation time. This is why the photon drag effect has been observed in rather limited number of semiconductors and
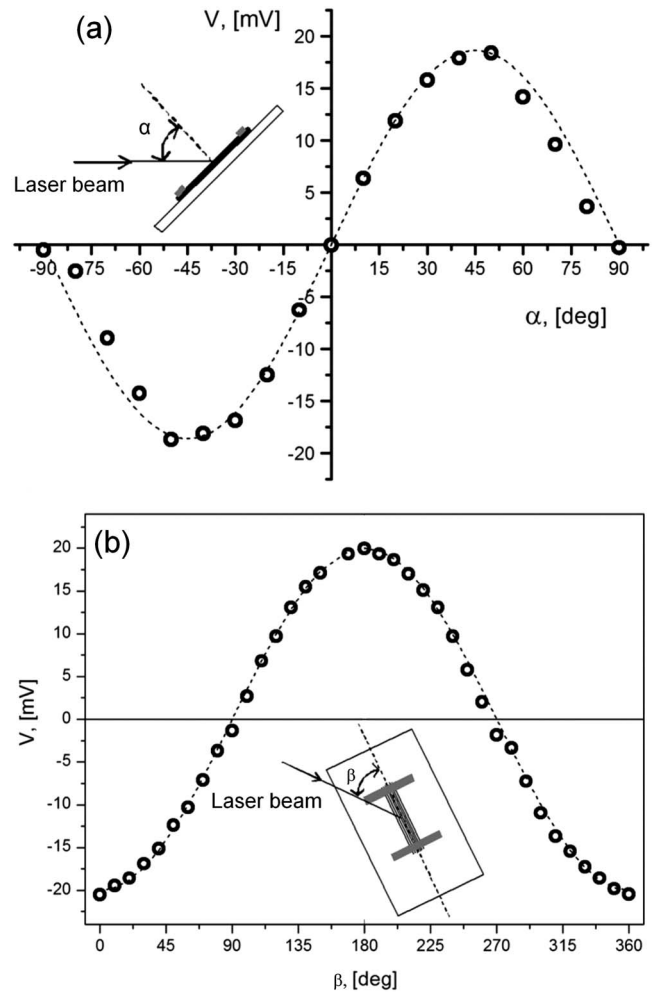

FIG. 3. The dependence of generated dc pulse amplitude (v) on (a) incidence angle α and (b) on azimuth angle, β measured at $\beta=0°$ and $\alpha=+50°$, respectively, at the laser pulse energy of 18 mJ. The experimental points are shown by open circles; dashed lines correspond to (a) $\sin 2\alpha$ and (b) $\cos \beta$.

semimetals where these conditions can be fulfilled for intraband transitions only.[17–20]

We believe that the photon drag effect in the MWNT yarns (see Fig. 3) as well as reported earlier dc response of nanographite films[12,13] is due to unique properties of these graphitic nanocarbon materials, in which ballistic or quasi-ballistic electron transport[21,22] ensures relatively long momentum relaxation time despite the strong electron-phonon coupling. It is also very important that the thickness of the MWNT yarns and nanographite crystallites[12,13] is much smaller than the light penetration length, i.e., all electrons beneath the irradiated area are dragged by photons. In contrary in bulk graphite, the photon drag current is generated in the irradiated only in the skin-layer-deep subsurface area, and hence it is short cut by highly conductive adjacent graphene layers.

A distinctive feature of graphitic materials is the near zero energy gap at the K point of the first Brillouin zone (e.g., see Ref. 23). Graphene is a zero-gap semiconductor, i.e., the Fermi energy of a single graphene sheet is located at $E=0$, and hence valence and conduction bands cross at the K point located on Brillouin zone edge. Near the K point, the electron energy (E) is a linear function of the momentum $\hbar k$ (see Fig. 4), and $E=\pm\hbar v_F|k|$, where $v_F \approx 10^6$ m/s is the
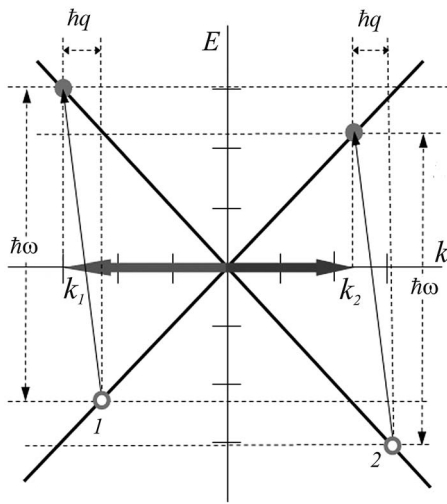
FIG. 4. Band structure of graphene in the vicinity of K point. Energy and momentum conservation imply that absorption of two photons of the same energy and momentum creates two electrons in the conduction band with different momenta, i.e., light-induced interband transitions produce electric current due to dragging of charge carriers by photons.

Fermi velocity. When several graphene sheets are stacked together, conduction and valence bands overlap. However, even in a bulk single graphite crystal, the band overlap is about 0.04 eV, i.e., the linear dependence of energy on electron momentum is still a good approximation to describe the light-induced effects in the visual and near-IR part of the spectrum.[23] Such a band structure facilitates the light-induced interband transitions in a wide spectral range in proximity of the K point, where the electron momentum is maximum. The momentum conservation implies that these transitions must be accompanied by the generation or absorption of phonons with large momenta. Since the energy gap at the Γ point of the Brillouin zone with zero value of the phonon and electron momentum is very large, interband transitions the edge K point dominant light absorption in the visual and near-IR part of the spectrum. This is a unique property of graphitic materials that manifest itself in the double resonance Raman scattering.[6–8]

In Fig. 4, we sketch light-induced transitions occurring in the electronic subsystem of graphitic material. The interaction of the nonequilibrium electrons with phonons takes place later and hence it is not shown here. Electron-hole pairs are created when energy $\hbar\omega$ of the incidence photon matches the energy gap between the valence and conduction bands, which cross at the Fermi level. The absorbed photon increases the electron momentum in the conduction band by the photon momentum $\hbar\boldsymbol{q}$. One can observe from Fig. 4 that in graphitic materials, absorption of two identical photons of the same energy and momentum is possible for two electrons moving in opposite directions in the conduction band. However, the total momentum of electrons generated due to light absorption will be nonzero, i.e., light-induced interband transitions produce electric current due to dragging of charge carriers by photons. The photon drag current can be detected by measuring voltage between electrodes attached to the sample. Although the appearance of the uncompensated carriers' momentum is possible in other materials, usually the photon drag current is very small to be detected because of high momentum relaxation rate. A relatively long momentum relaxation time for intersubband transitions in some semicon-

ductors has made it possible to observe the photon drag effect in the far IR region.[15–20] However, in carbon nanotubes, graphene, and similar graphitic nanocarbon materials, ballistic conductivity and moderate momentum relaxation rate are expected for nonequilibrium free electron carriers[21,22] generated by absorption of photons with energies in the visual and near-IR spectral range.[13]

To conclude, in graphitic materials, a unique combination of the strong electron-phonon coupling, quasiballistic electron transport, and small thickness give rise to efficient momentum transfer in a wide spectral range that spans from far IR to ultraviolet. The resulting drag of quasiballistically propagating electrons dominates in the experimentally observed optoelectronic phenomenon. The measured ratio of the dc voltage to the laser power of 750 mV/MW at the wavelength of 1600 nm makes carbon nanotube yarns promising, in particular, for visualization the temporal profile, polarization, and propagation direction of the laser pulse. Very wide spectral range of light absorption in the graphitic nanomaterials makes them attractive for conversion of the optical radiation energy into electricity especially because the conversion efficiency can be enhanced, e.g., in multipass geometry.

[1] Ph. Avouris, Zh. Chen, and V. Perebeinos, Nat. Nanotechnol. **2**, 605 (2007).
[2] Ph. Avouris, M. Freitag, and V. Perebeionos, Nat. Photonics **2**, 341 (2008).
[3] Zh. Zhong, N. M. Gabor, J. E. Sharping, A. E. Gaeta, and P. L. McEuen, Nat. Nanotechnol. **3**, 201 (2008).
[4] X. Du, I. Skachko, A. Barker and Y. Andrei, Nat. Nanotechnol. **3**, 491 (2008).
[5] F. Keummeth, S. Ilani, D. C. Ralph, and P. L. McEuen, Nature (London) **452**, 448 (2008).
[6] C. Thomsen and S. Reich, Phys. Rev. Lett. **85**, 5214 (2000).
[7] A. C. Ferrari, J. C. Meyer, V. Scardachi, C. Casiraghi, M. Lazzeri, F. Mauri, S. Piscanec, D. Jiang, K. S. Novoselov, S. Roth, and A. K. Geaim, Phys. Rev. Lett. **97**, 187401 (2006).
[8] R. Pfeiffer, H. Kuzmany, F. Simon, S. N. Bokova, and E. D. Obraztsova, Phys. Rev. B **71**, 155409 (2005).
[9] R. Loudon, S. M. Barnett, and C. Baxter, Phys. Rev. A **71**, 063802 (2005).
[10] M. Zhang, K. R. Atkinson, and R. H. Baughman, Science **306**, 1358 (2004).
[11] Y. R. Shen, *Principles of Nonlinear Optics* (Wiley-Interscience, New York, 1984).
[12] G. M. Mikheev, R. G. Zonov, A. N. Obraztsov, and Yu. P. Svirko, Appl. Phys. Lett. **84**, 4854 (2004).
[13] A. N. Obraztsov, G. M. Mikheev, Yu. P. Svirko, R. G. Zonov, A. P. Volkov, D. A. Lyashenko, and K. Paivasaari, Diamond Relat. Mater. **15**, 842 (2006).
[14] J. L. W. Siders, S. A. Trugman, F. H. Garzon, R. J. Houlton, and A. J. Taylor, Phys. Rev. B **61**, 13633 (2000).
[15] A. A. Grinberg and S. Luryi, Phys. Rev. B **38**, 87 (1988).
[16] J. E. Goff and W. L. Schaich, Phys. Rev. B **61**, 10471 (2000).
[17] V. I. Vladimirov, S. L. Pyshkin, and N. A. Ferdman, JETP Lett. **9**, 28 (1969).
[18] A. M. Danishevsky, A. A. Kastalsky, S. M. Ryvkin, and I. D. Yaroshevsky, Sov. Phys. JETP **58**, 544 (1970).
[19] S. Panyakeow, J. Shirafuji, and Y. Inuishi, J. Appl. Phys. **46**, 1245 (1975).
[20] S. Marchetti and R. Simili, Phys. Scr. **37**, 820 (1988).
[21] C. Berger, Y. Yi, Z. I. Wang, and W. A. de Heer, Appl. Phys. A: Mater. Sci. Process. **74**, 363 (2002).
[22] H. J. Li, W. G. Lu, J. J. Li, X. D. Bai, and C. Z. Gu, Phys. Rev. Lett. **95**, 086601 (2005).
[23] B. Partoens and F. M. Peeters, Phys. Rev. B **74**, 075404 (2006).